# An ultra-thin waveguide twist constructed using fish-scale metallic wires

Jin Han,[1,2] Hongqiang Li,[1,2,a)] Yuancheng Fan,[1,2] Zeyong Wei,[1,2] Chao Wu,[1,2] Yang Cao,[1,2] Xing Yu,[1,2] Fang Li,[1,2] and Zhanshan Wang[1,2]

[1)] *Department of Physics, Tongji University, Shanghai 200092, People's Republic of China*

[2)] *Shanghai Key Laboratory of Special Artifical Microstructure Materials and Technology, Shanghai, People's Republic of China*

This study theoretically and experimentally investigates the transmission properties of a metamaterial slab comprised of two layers of metallic fish-scale structure arrays and a sandwiched dielectric layer. Calculations show that the asymmetric transmission can be tuned by varying the slab thickness, due to evanescent interlayer coupling. The spatial evolution of the local field inside the structure indicates that the slab functions as a perfect polarization transformer at certain frequencies in the manner of a waveguide twist. Measured transmission spectra are in good agreement with calculated results when material dissipation is considered.

Recently, considerable interests in the asymmetric transmission (AT) of polarized light has been revived in the context of planar chiral metamaterials[1–8].This phenomenon, arising from the vector nature of electromagnetic waves, still satisfies the de Hoop reciprocity as revealed by Jones and Muller matrix formulation[9]. That is, in the transfer-matrix representation of an optical system, the matrix for reverse transmission is the transpose of that of forward transmission. The system will give rise to asymmetric transmission of polarized light provided that the system is chiral and anistropic[7]. The metamaterial approach[1–9] enables this functionality to be implemented at subwavelength thicknesses. These findings constitute an alternative solution for one-way electromagnetic isolator and related devices to the scheme relying on nonreciprocal ingredients such as gyrotropy[10], or nonlinearity[11]et al.

It is notable that the coupling among the metallic building blocks or meta-atoms is instrumental for the exotic properties of the metamaterial. A microscopic investigation is helpful for deeper insight into the underlying physics as well as for practical applications. Fish-scale metallic wire[12], taken as a typical example of a planar chiral metamaterial, has been investigated extensively as an optical magnetic mirror[13] and local field concentrator[14]. In this paper, we propose a device for asymmetric transmission that is composed of two layers of fish-scale structure metallic wires in an orthogonal arrangement and a sandwiched dielectric spacer layer. Calculation of the local field distribution reveals that the thin slab functions as a waveguide twist[15,16], giving rise to nearly perfect asymmetric transmission. This physical picture unifies mode matching at the entrance interface and polarization transformation inside the slab to explain the formation of AT and its dependence on slab thickness.

A unit cell of our model slab, shown in front view and stereogram in Fig. 1(a) and Fig. 1(b), is composed of circularly meandering and straight metallic strips. The metallic patterns on the front and back surfaces of the dielectric layer are the same, but are rotated relative to each other at an angle of $90^0$ about the $z$ axis. The geometric parameters marked in Fig. 1(a) are the width $w = 1.4$mm of the metallic strips, the radii $r_1 = 3.05$mm, $r_2 = 4.45$mm of the inner and outer circles, the length $a = 4.8$mm of the straight metallic strip, and period $p =$ 15mm of a square unit cell. The substrate has a thickness of $t = 1.8$mm. Fig. 1(c) shows a photo of our sample with the same geometric parameters as the theoretical model in Fig. 1(a). The metallic fish-scale patterns are fabricated and deposited on the $35\mu m$-thick copper foils on both sides of an FR4 dielectric substrate. The lateral size of the entire sample slab is $570 \times 435$mm.

We perform finite-difference-in-time-domain (FDTD) numerical simulations to calculate the transmission spectra of our fish-scale model for $x$-polarized and $y$-polarized incident waves along the $+z$ and $-z$ directions. For simplicity, metals are assumed to be perfect electric conductors (PECs). The dielectric substrate is assumed to be lossless, with a permittivity $\epsilon_r \approx 4.1$, the same as that of the FR4 substrate. The transmission coefficient $T^d_{ij}$ is defined in terms of the intensity of the electric field, with the first and the second subscripts denoting the polarized states of the incident wave and transmitted wave components, respectively, and the superscript $d = +/-$ referring to forward(+) or backward(−) transmission. For example, $T^+_{xy}$ denotes the normalized intensity of the $y$-polarized transmitted wave component($\vec{E} \parallel \vec{y}$) with respect to the $x$-polarized($\vec{E} \parallel \vec{x}$) incident wave along the forward direction ($k_z$>0 and $k_\parallel$=0), and the total transmissivity (for all polarizations) is given by $\mid T^+_{xx} + T^+_{xy} \mid$.

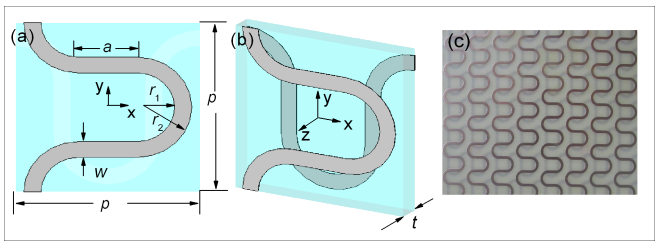


FIG. 1. a schematic of (a)the front view (in $x - y$ plane) of the sample slab, (b)the stereogram of a unit cell, (c)a photo of our sample. The thickness of the dielectric layer is $t$ =1.8mm.

[a)] Electronic mail: hqlee@tongji.edu.cn

Fig. 2(a) and Fig. 2(b) presents the forward and backward transmission spectra $T^+$ and $T^-$ of our model slab calculated by the FDTD algorithm. We see, both in Fig. 2(a) and Fig. 2(b) that $T_{xx}$ is nearly superposed onto $T_{yy}$. This is because the structure, taken as a whole, is essentially isotropic, due to the orthogonal alignment of the fish-scale patterns on both sides of the dielectric layer. However, a salient feature in Fig. 2(a) and Fig. 2(b) is that $T_{xy}$ is markedly different from $T_{yx}$ at all frequencies. $T_{xy}$ and $T_{yx}$ are interchanged when the incident direction (wavevector $\vec{k}$) is reversed, giving rise to a clear signature of asymmetric transmission. A maximum of 97% transmission is reached at 8.7GHz in the spectrum of $T^+_{xy}$; meanwhile, both $T^+_{yx}$ and $T^+_{xx}$ are below 1% transmission near 8.7GHz.

The asymmetric property described above has close connections with the transmission spectra of a monolayer of fish-scale metallic wires. As shown in Fig. 2(c), the monolayer with $y$-oriented wires is transparent to the $y$-polarized incident wave ($T_{yy}$>60%) around 8.7GHz but opaque to the $x$-polarized incident wave ($T_{xx}$<10%) at the same frequencies. This is because there exists a local mode owned by the $x/y$-oriented fish-scale structure that only couples to $x/y$-polarized plane waves near the frequency 8.7GHz[12]. In the case presented in Fig. 2(a), an $x$-polarized incident wave at approximately 8.7GHz in the forward direction will meet the $x$-oriented fish-scale patterns first, so that it can propagate inside the slab and be transformed into $y$-polarization afterwards. In contrast, an $y$-polarized incidence at the same frequency can not couple with the local mode based on the metallic layer at the entrance. Similar rules also apply to a backward incident wave along the $-z$ direction, as seen by interchanging $x$ and $y$ subscripts (see Fig. 2(b)). However, asymmetric transmission with high bandwidth, as shown in Fig. 2(a) and Fig. 2(b), can not be deduced from the transmission properties of a monolayer of fish-scale metallic patterns (Fig. 2(c)). The coupling between the metallic layers must be considered for a complete description of theses phenomena.

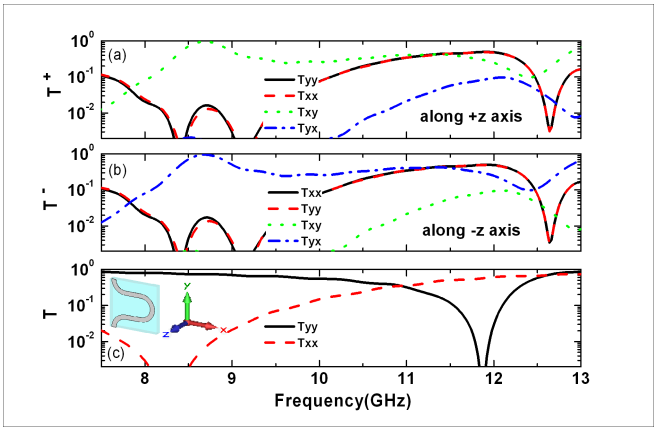


FIG. 2. Calculated transmission spectra for $x$-polarized ($\vec{E} \parallel \vec{x}$) and $y$ polarized ($\vec{E} \parallel \vec{y}$) incidence of our sample slab (a)along $+z$ direction and (b) along $-z$ direction. (c)a monolayer of fish-scale structure metallic arrays with $y$-oriented wires shown in Fig. 1(a).

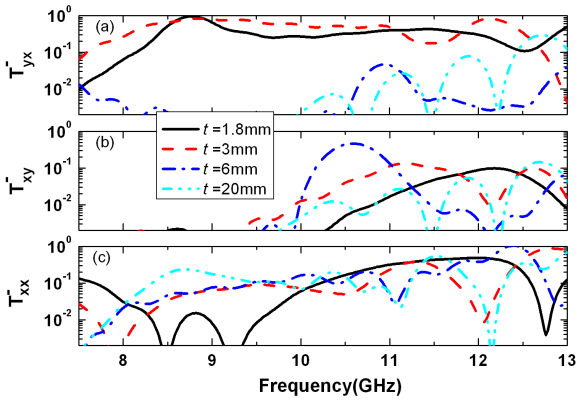


FIG. 3. The spectra of backward transmission for different slab thicknesses $t$.

Fig. 3 presents the calculated transmission spectra $T^-_{yx}$, $T^-_{xy}$ and $T^-_{xx}$ with respect to the different thicknesses $t$ = 1.8mm, 3mm, 6mm and 20mm of the dielectric layer. We see from Fig. 3(a) that, $T^-_{yx}$ varies rapidly in lineshape as a function of slab thickness $t$. When $t$ is small, both $T^-_{xx}$ and $T^-_{xy}$ are suppressed very well at a level of $10^{-2} - 10^{-3}$, within the 7.5−10GHz range, giving rise to an AT functionality with good performance. At $t$ = 6mm, the AT below 10GHz disappears. However, AT is observed along the reverse direction near 10.5GHz where $T^-_{xy}$ reaches its maximum of 0.46, and $|T^-_{yx}+T^-_{xx}| \approx$ 0.027 is still very small. This means that the asymmetric transmission can be tuned to a different frequency even along the reversed direction, by changing the thickness $t$. For much larger values of $t$, such as $t$ = 20mm, the evanescent interlayer coupling is negligible and the AT effect disappears at all frequencies.

A direct way to witness the formation of asymmetric transmission is to observe the evolution of wave fields propagating inside the model slab. The snapshots in Fig. 4 calculated using the FDTD algorithm show that, for backward transmission at 8.7GHz, the outgoing waves are always $x$-polarized (see Fig. 4(e), (j)) even when the incident wave is $y$-polarized (Fig. 4(f)). This is because only the $x$-polarized wave component at 8.7GHz is allowed to pass through the $x$-oriented fish-scale metallic arrays at the outgoing surface. We see from Fig. 4(b)-(d) and Fig. 4(g)-(i) that the field patterns are twisted inside the slab as a consequence of interlayer coupling. We also see that the field strength inside the slab remains high (Fig. 4(c)), even when the incident wave is blocked at the entrance surface. These are the features of evanescent coupling between metallic layers. The picture demonstrates that our model slab can function as

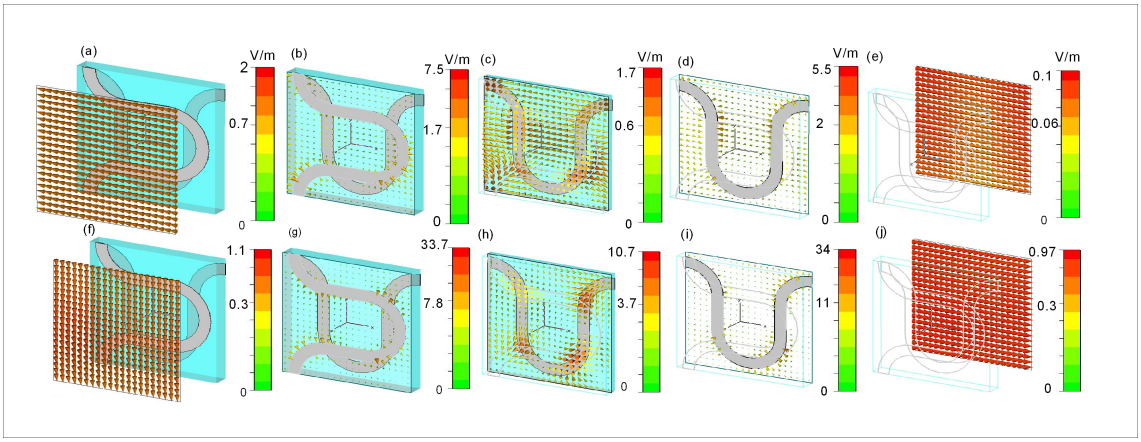


FIG. 4. Snapshots of the electric field strength at different $z$ coordinates for $x$-polarized ((a)-(e)) and $y$-polarized ((f)-(j)) incident plane waves along the $-z$ direction. (a) and (f): at $z = 7.4$mm of the incoming regime; (b) and (g): at $z = 0$ of the front surface(entrance); (c) and (h) at $z = -1.1$mm within the dielectric layer; (d) and (i) at $z = -1.8$mm of the backside surface; (e) and (j): at $z = -8.4$mm of the outgoing regime. The local field strength, as illustrated by the color bar, is normalized to that of the incident wave.

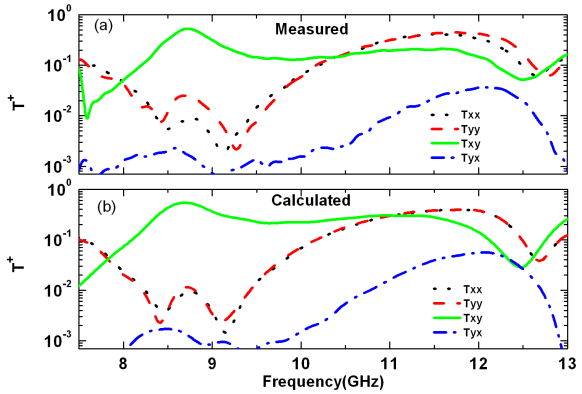


FIG. 5. (a) measured and (b) calculated forward transmission of our sample slab.

an ultra-thin polarization transformer just as a waveguide twist with $90^0$ orientation would function.

The transmission spectra through our sample (see Fig. 1(c)) were measured with a vector network analyzer (Agilent 8722ES) in an anechoic chamber. The spectra for forward transmission are shown in Fig. 5(a). A peak value of 0.53 was measured at 8.7GHz in the spectrum of $T_{xy}$. Measurements are quantitatively verified by calculations (see Fig. 5(b)) adopting a complex permittivity of $\epsilon_r \approx 4.1 + 0.1i$ for the FR4 substrate. Almost half of the wave energy is removed by the absorption channel (not shown) due to a strong enhancement of the local field inside the slab, which maximizes dielectric dissipation. The reflection at 8.7GHz is still very small.

In conclusion, we provide a picture of waveguide twist to explain the AT effect of our model slab, which contains two layers of fish-scale metallic wires. Calculations on the AT with respect to different slab thicknesses and the spatial evolution of the local field verifies that near-field interlayer coupling enables the polarization transformation of the outgoing waves, whereas the linearly polarized incident wave can only propagate into the slab in one direction, giving rise to one-way asymmetric transmission. Our findings are beneficial for the design of optical isolators based on planar chiral metamaterials. This work was supported by NSFC (No. 10974144, 60674778), the National 863 Program of China (No. 2006AA03Z407), NCET (07-0621), STCSM, and SHEDF (No. 06SG24).

[1]V. A. Fedotov, A. S. Schwanecke, N. I. Zheludev, V. V. Khardikov, and S. L. Prosvirnin, Nano Lett. **7,** 1996 (2007).
[2]E. Plum, V. A. Fedotov, and N. I. Zheludev, Appl. Phys. Lett. **94,** 131901 (2009).
[3]S. V. Zhukovsky, A. V. Novitsky, and V. M. Galynsky, Opt.Lett. **34,** 1988 (2009).
[4]E. Plum, V. A. Fedotov, and N. I. Zheludev, arXiv.org.1006.0870 (2010).
[5]R. Singh *et al.*, Phys. Rev. B. **80,** 153104 (2009).
[6]S. I. Maslovski, D. K. Morits, and S. A. Tretyakov, J. Opt. A: Pure Appl. Opt. **11,** 074004 (2009).
[7]V. A. Fedotov, P. L. Mladyonov, S. L. Prosvirnin, A. V.Rogacheva, Y. Chen, and N. I. Zheludev, Phys. Rev.Lett. **97,** 167401 (2006).
[8]C. Menzel, C. Helgert, C. Rockstuhl, E.-B. Kley, A. Tunnermann, T. Pertsch, and F. Lederer, Phys.Rev.Lett. **104,** 253902 (2010).
[9]R. J. Potton, Rep. Prog. Phys.**67,** 717 (2004).
[10]V. M. Agranowitz and V. L. Ginzburg, Spatial Dispersion in Crystal Optics and the Theory of Excitons (Wiley:London)(1966)
[11]Y. Fan, J. Han, Z. Wei, C. Wu, Y. Cao, X. Yu, and H. Li, arXiv.org.1012.2252 (2010).
[12]V. A. Fedotov, P. L. Mladyonov, S. L. Prosvirnin, and N. I. Zheludev, Phys. Rev. E. **72,** 056613 (2005).
[13]A. S. Schwanecke *et al.*, J. Opt. A: Pure Appl. Opt. **9,** L1-L2 (2007).
[14]T. S. Kao *et al.*, Appl. Phys. Lett. **96,** 041103 (2010).
[15]H. A. Wheeler, and H. Schwiebert, IRE Trans. Microwave Theory Tech. **MTT-3,** 44(1955).
[16]B. C.DeLoach,IRE Trans. Microwave Theory Tech. **MTT-9,**130 (1961).